Supporting Information

Facile synthesis of fluorescent probe based on Terbium-based metal-organic framework for selective detection of Fe(III) and Al(III)

Xuequan Jing[a,b,c], Jiaming Liu[a,b,c], Meina Guo[a,b,f], Guoliang Chen[a,d], Guoqing Ren[e], Jiarong Li[a,b,c], Haonan Qin[a,b,c], Zhangwei Yao[a,b,c], Yinhua Wan[a,b,c,f,g], Weijie Song[a,b,c,f,g], Huifeng Zeng[a,b,f], Feifei Yang[a,b,f], Da Zhao[a,b,f], Kang Hu[a,b,c,f,*]

[a]Ganjiang Innovation Academy, Chinese Academy of Sciences, Ganzhou 341000, P. R. China

[b]Key Laboratory of Rare Earth, Chinese Academy of Sciences, Ganzhou 341000, P. R. China

[c]School of Rare Earths, University of Science and Technology of China, Hefei, Anhui 230026, P. R. China

[d]China Rare Earth Group Co., Ltd, Ganzhou 341000, P. R. China

[e]Jiangxi ECO-ADVANCE Technology Co., LTD, Ganzhou 341000, P. R. China

[f]Jiangxi Province Key Laboratory of Cleaner Production of Rare Earths, Ganzhou 341000, P. R. China

[g]Institute of Process Engineering, Chinese Academy of Sciences, Beijing 100190, P. R. China

*Corresponding author. E-mail address: hukang0602@126.com (K. Hu)

Keywords: selective detection; metal-organic framework; ferric ions (Fe^{3+}); aluminum ions (Al^{3+})

Table S1 The comparison between fluorescent probe for selective detection of Fe^{3+} and Al^{3+} prepared in this work with partial updated reported literatures.

Probe	Chemicals	Synthetic conditions	Detection limits	Linear range	Ref.
4-HMP-PDI	N,N'-bis(hexyl)1,7-dibromoperylenetetracarboxylic diimide, 4-pyridinemethanol, K_2CO_3 and DMF	120-130 °C for 7 h under N_2 atmosphere, monitored by TLC, under vacuum, purified by silica column with hexane.	36.52 ppb of Fe^{3+} 43.12 ppb of Al^{3+}	0 ppm to 4.95 ppm of Fe^{3+} 0 ppm to 3.24 ppm of Al^{3+}	1
Perylenetetracarboxylicdiimide fluorophore with an amine unit	$Pd_2(dba)_3$, 2,2' bis(diphenylphosphino)-1,1'-binaphthalene, toluene, 1-adamantlyamine, dibromo-PDI, sodium tert-butoxide and diethyl ether	stirred for 30 min at room temperature, stirred for 24 h at 100°C.	2.16 µM of Fe^{3+} 3.47µM of Al^{3+}	0 µM to 20 µM for Fe^{3+} 0 µM to 20 µM for Al^{3+}	2
Rhodamine-thiophene-based fluorogenic probe	N-(Rhodamine-6G) lactam-ethylenediamine (LA), thiophene-2-carboxylic acid, EDC, 4-dimethylamino pyridine and CH_2Cl_2.	stirred at room temperature for 12 h, washed with water and concentrated in a vacuum, purified by chromatography.	5 µM of Fe^{3+} 6 µM of Al^{3+}	----	3
Förster resonance energy transfer (FRET)-based fluorescent probe	rhodamine hydrazide, absolute methanol, 4-pyridinecarboxaldehyde, $NaHCO_3$ and CH_2Cl_2	dried over anhydrous Na_2SO_4 and evaporated using rotary evaporator, purification by column chromatography	----	35 µM to 115 µM for Fe^{3+}	4
Cadmium-based 3D luminescent MOF ($[Cd_2(SA)_2(L)_2 \cdot H_2O]_n$)	$Cd(NO_3)_2 \cdot 4H_2O$, succinic acid, 3,3'-azobis(pyridine) and DMF	stirred for 1-2 h, kept for crystallization at ambient temperature for 15-18 days.	2.4 µM of Fe^{3+} 9.3 µM of Al^{3+}	2 µM to 20 µM for Fe^{3+} 2 µM to 20 µM for Al^{3+}	5
A trichromatic and white-light-emitting MOF composite	H_2L, $ZnBr_2$, DMF and H_2O	heated at 105 °C for 24 h, collected by filtration, washed with DMF and dried in air.	0.41 ppm of Fe^{3+} 0.12 ppm of Al^{3+}	0 to 1.50 mM for Fe^{3+} 0 to 1.50 mM for Al^{3+}	6

PYTG based on pyrene and a C_3-symmetric triaminoguanidinium core	Triaminoguanidinium chloride, ethanol, H_2O and pyrene-1-carboxaldehyde	stirred and refluxed for 12 h at 85°C, filtered and washed 3 times with diethyl ether.	5.4 nM of Fe^{3+} 14 nM of Al^{3+}	0.5 µM to 3 µM for Fe^{3+} 30 µM to 80 µM for Al^{3+}	7
2-(((4-(9H–carbazol-9-yl)phenyl)imino)methyl)-5-(diphenylamino) phenol (para-CPDP)	3-OH TPA aldehyde, methanol solution, Pd/C, $NaBH_4$, carbazole, CH_3CN, sodium hydride, 2-/4-fluoronitrobenzene	stirred for 4 h at room temperature, stirred for another 2 h, the reaction mixture was refluxed for overnight.	10 µM of Fe^{3+} 500 µM of Al^{3+}	2.5 µM to 15 µM for Fe^{3+} 2.5 µM to 15 µM for Al^{3+}	8
Cd(II)-based MOF	$Cd(NO_3)\cdot 6H_2O$, PAM, 4-bpdb, DMF and H_2O	heated at 100°C under autogenous pressure for 4 days	0.3 µM of Fe^{3+} 0.56 µM of Al^{3+}	0 µM to 16 µM for Fe^{3} 0 µM to 50 µM for Al^{3+}	9
Organic gelator (WJ) based on benzimidazole and acylhydrazone naphthol moities	N-methoxycarbonylmethyl-2-undecyl-1H-benzimidazole, EtOH, hydrazine, 2-hydroxy naphthalene formaldehyde, acetic acid and DMF	stirred under reflux for 10 h at 80°C, heated at 80°C for 8 h.	0.00381 µM of Fe^{3+} 0.0578 µM of Al^{3+}	40 µM to 160 µM for Fe^{3} 1 µM to 3 µM for Al^{3+}	10
Schiff-base (HL) based on rhodamine B	(4-Hydroxybenzoyl)hydrazine, rhodamine B, methanol, hydrazine hydrate	removed under reduced pressure, washed with deionized water and dried under reduced pressure.	0.14 µM of Fe^{3+} 0.22 µM of Al^{3+}	20 µM to 22 µM for Fe^{3} 20 µM to 22 µM for Al^{3+}	11
Zn(II)-coordination polymer	$Zn(NO_3)_2\cdot 6H_2O$, H_3ClP, pbt, H_2O and DMF	kept at 120 °C for 3 days	3.3 ppm of Fe^{3+} 0.764 ppm of Al^{3+}	0 µM to 150 µM for Fe^{3} 75 µM to 425 µM for Al^{3+}	12
Nitrobenzoxadiazole-Appended Calix[4] arene Conjugate (L)	Precursors P2, P3 and 4-chloro-7-nitrobenzo-2-oxa-1,3-diazole (NBD-Cl), dichloromethane and triethylamine	stirred for 48 h, checked by TLC using 50% ethyl acetate in petroleum ether, purified by column chromatography.	1.7 ppm of Fe^{3+} 2.3 ppm of Al^{3+}	0 µM to 3 µM for Fe^{3} 0 µM to 2 µM for Al^{3+}	13

Co(II) metal-organic framework	$CoCl_2 \cdot 6H_2O$, H_4L, phen and CH_3CN	heated at 140°C for 3 days.	1.79 µM of Fe^{3+} 35.4 µM of Al^{3+}	0 µM to 600 µM for Fe^3 126 µM to 1.26 mM for Al^{3+}	14
A novel colorimetric Schiff-base receptor	2-amino-3-methylpyridine, absolute ethanol, 2-hydroxy-5-((2-nitrophenyl) diazenyl) benzaldehyde and triethylamine	heated in a water bath for 3 h, separated and washed with hot EtOH.	4.98 µM of Fe^{3+} 4.03 µM of Al^{3+}	----	15
A cation chemoprobe bearing naphthol O-H and imine group	2-hydroxy-1-naphthaldehyde, 5-methyl-2-amine pyridine and ethanol	heated at 60°C for 5 hours	0.1 µM of Fe^{3+} 0.43 µM of Al^{3+}	0 µM to 100 µM for Fe^3 0 µM to 100 µM for Al^{3+}	16
A fluorescent-colorimetric chemosensor based on a Schiff base	2-hydroxy-1-naphthaldehyde, 5-aminosalicylic acid and ethanol	70°C for 24 h	0.358 µM of Fe^{3+} 0.489 µM of Al^{3+}	2 µM to 20 µM for Fe^{3+} 2 µM to 7 µM for Al^{3+}	17
A naphthylamide based fluorescent chemosensor	TPP, TBAB, 1-hydroxy-2-naphthoic acid, 1,2-phenylenediamine and methanol	heated in an oil bath at 120°C for 1 h, stirred for 30 min	0.0352 µM of Fe^{3+} 5.022 µM of Al^{3+}	0 µM to 200 µM for Fe^3 0 µM to 80 µM for Al^{3+}	18
A pillar-like 3D lanthanide-organic framework (Eu-MOF)	H_4L, $Eu(NO_3)_3 \cdot 6H_2O$, $NaAc \cdot 3H_2O$, Hac and H_2O	190°C for 48 h	0.39 µM of Fe^{3+} 0.084 µM of Al^{3+}	0.01 µM to 220 µM for Fe^3 0 µM to 500 µM for Al^{3+}	19
2,6-diaminopyridine-coupled rhodamines	2,6-diaminopyridine, rhodamine acid chloride, ammonium formate, acetonitrile	reflux 4 h, reaction 10 h, reflux 10 h	2.79 µM of Fe^{3+} 2.43 µM of Al^{3+}	120 µM to 180 µM for Fe^3 60 µM to 100 µM for Al^{3+}	20
Zn(II)-based MOF	$Zn(NO_3)_2 \cdot 6H_2O$, H_2DHT, BPP, DMF and H_2O	heated at 150 °C for 48 h	0.446 µM of Fe^{3+} 0.269 µM of Al^{3+}	0 µM to 7 µM for Fe^3 0 µM to 40 µM for Al^{3+}	21

A tetraphenyl ethylene-based zinc complex	2-bromo-1,1,2-triphenylethylene, pyridine-4-boronic acid, tetrabutylammonium bromide, $Pd[P(C_6H_5)_3]_4$, K_2CO_3, DMF, dimethyl-5-(bromomethyl) isophthalate, acetonitrile, HCl, $ZnCl_2$, acetonitrile and H_2O	stirred under an N_2 atmosphere at 100°C for 24 h, 100°C for 12 h, heated at 120°C for 3 days	0.31 μM of Fe^{3+} 0.913 μM of Al^{3+}	0 μM to 40 μM for Fe^3 0 μM to 40 μM for Al^{3+}	22
A brand-new Cd^{II}-based MOF (JXUST-18)	$Cd(NO_3)_2 \cdot 4H_2O$, BTBD, H_2AIC, N,N-dimethylformamide (DMF) and deionized water	ultrasonic processing for 2 min and stirring for 10 min, heated to 120°C for one day.	0.196 μM of Fe^{3+} 0.184 μM of Al^{3+}	0 μM to 10 μM for Fe^3 0 μM to 5 μM for Al^{3+}	23
Terbium-based MOF	$Tb(NO_3)_3 \cdot 6H_2O$, 5-aminoisophthalic acid, DMF, H_2O and ethanol	heated at 150°C for 12 h; washed three times.	0.91 μM of Fe^{3+} 6.1 μM of Al^{3+}	0 μM to 400 μM for Fe^3 0 μM to 1.0 mM for Al^{3+}	This work

Table S2 The specific surface areas of Tb-MOF before and after recognizing Al^{3+}.

Sample	S_{BET} (m^2g^{-1})	S_{BJH} (m^2g^{-1})	V_{total} (cm^3g^{-1})	$D_{average}$ (nm)
Tb-MOF	8.06	4.79	0.048	15.27
Tb-MOF+Al^{3+}	16.54	14.95	0.056	17.90

S_{BET}: BET surface area, S_{BJH}: BJH adsorption cumulative surface area of pores, V_{total}: Total volume in pores, $D_{average}$: BJH adsorption average pore diameter.

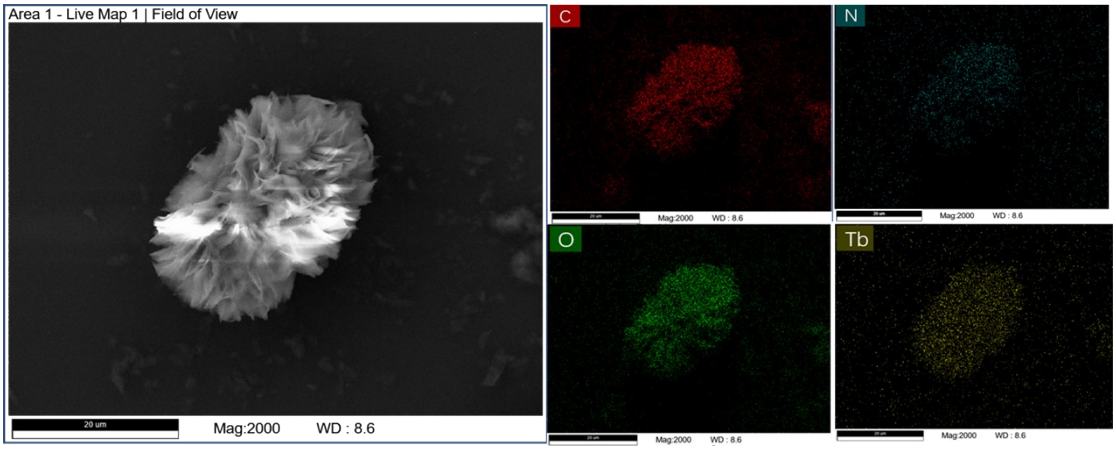

Fig. S1 Scanning electron microscope (SEM) images and EDS elemental mappings of Tb-MOF.

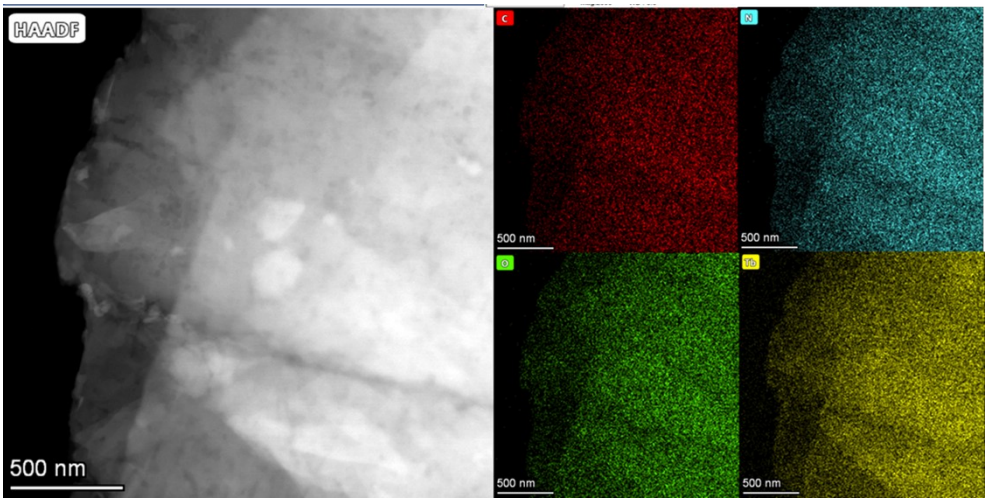

Fig. S2 High-angle annular dark-field scanning transmission electron microscopy (HAADF-STEM) images and EDS elemental mappings of Tb-MOF.

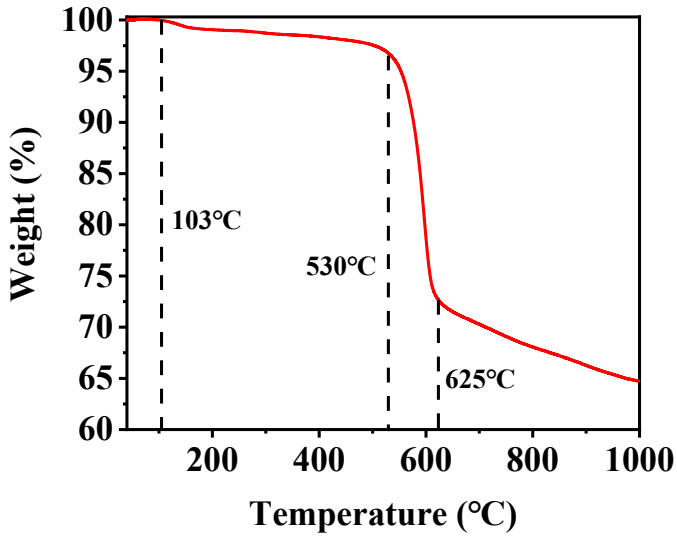

Fig. S3 Thermal gravimetric analysis for Tb-MOF.

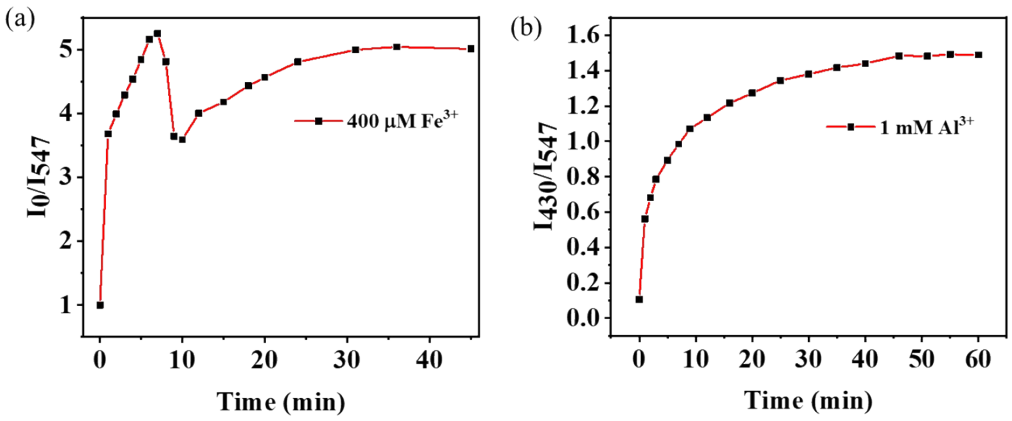

Fig. S4 (a) Time-dependent emission spectra for the Tb-MOF in aqueous solution containing 400 μM Fe^{3+}; (b) Time-dependent emission spectra for Tb-MOF in aqueous solution containing 1.0 mM Al^{3+}.

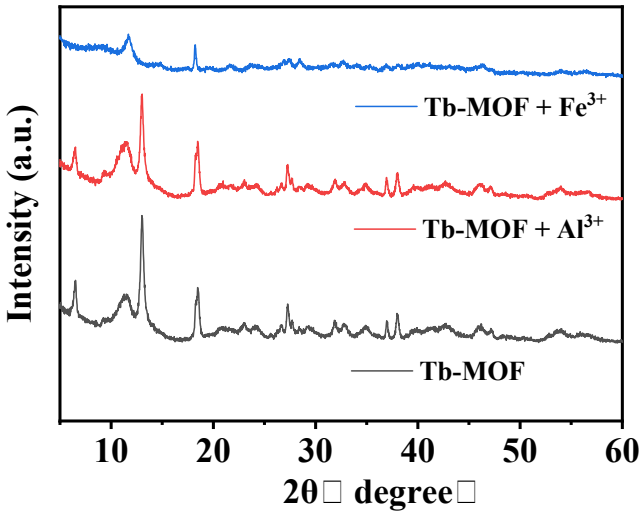

Fig. S5 XRD spectra before and after Tb-MOF identifying Fe^{3+} and Al^{3+}.

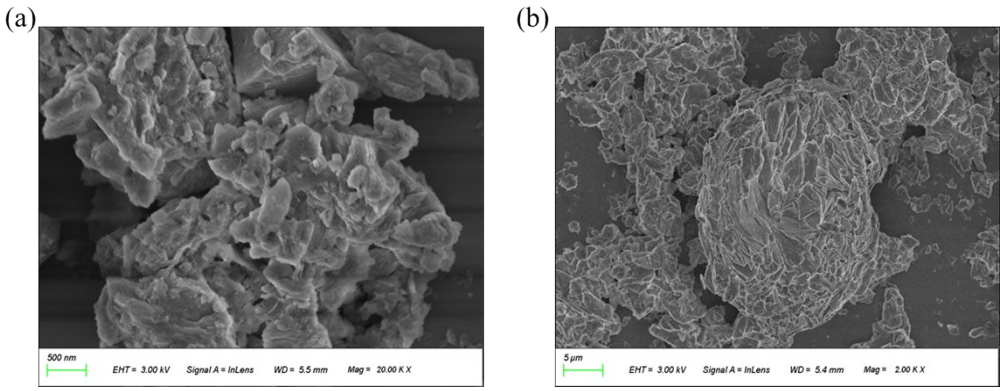

Fig. S6 The SEM images of Tb-MOF after recognizing (a) Fe^{3+} and (b) Al^{3+}.

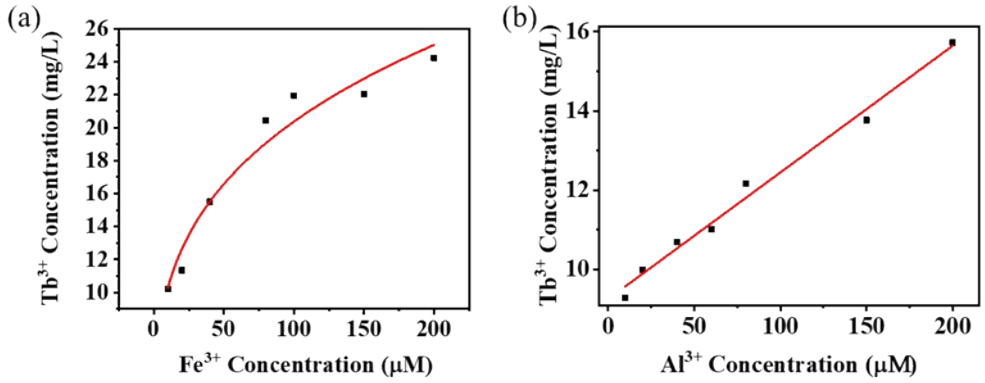

Fig. S7 Tb^{3+}concentration changes in the presence of Fe^{3+} and Al^{3+} at different concentrations.

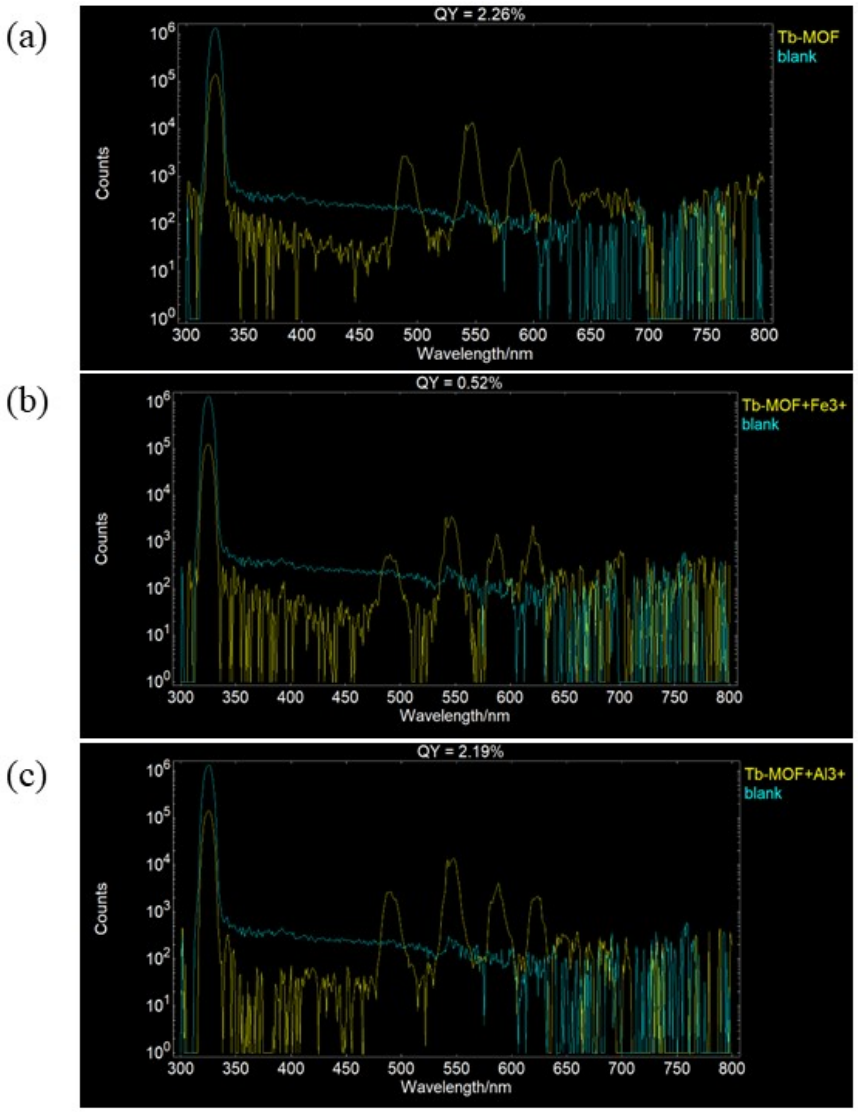

Fig. S8 Quantum yield of (a) Tb-MOF; (b) Tb-MOF after recognizing Fe^{3+}; (c) Tb-MOF after recognizing Al^{3+}.

(a)

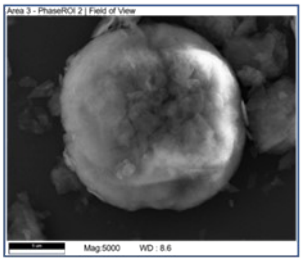

(b)

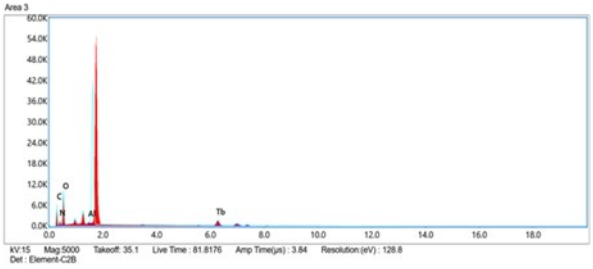

(c)

Element	Weight %	Atomic %	Error %	Net Int.	K Ratio	Z	A	F
C K	16.12	34.99	7.91	353.34	0.0813	1.2787	0.3947	1.0000
N K	6.30	11.74	10.48	94.85	0.0200	1.2500	0.2541	1.0000
O K	27.66	45.09	8.58	706.48	0.1068	1.2247	0.3152	1.0000
Al K	0.00	0.00	99.99	0.01	0.0000	1.0922	0.4646	1.0022
Tb L	49.91	8.19	4.97	258.06	0.3618	0.7004	1.0346	1.0005

Fig. S9 EDS analysis of Tb-MOF after recognizing Al^{3+}.

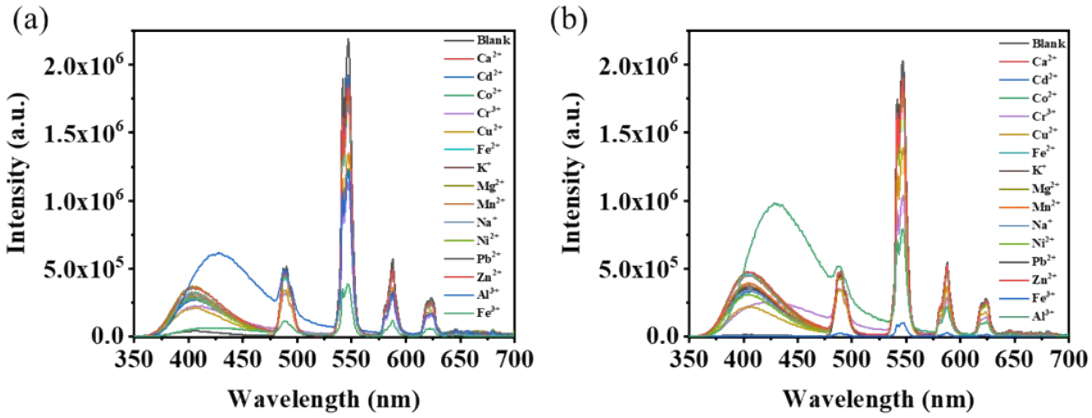

Fig. S10 Fluorescence spectra of Tb-MOF in different metal ion solutions.

Notes and references

1. A. Kundu, J. Pitchaimani, V. Madhu, P. Sakthivel, R. Ganesamoorthy and S. P. Anthony, *Journal of Fluorescence*, 2017, **27**, 491-500.
2. S. Suganya, J. W. Namgoong, A. K. Mutyala, S. Velmathi, J. P. Kim and J. S. Park, *Journal of Photochemistry and Photobiology A: Chemistry*, 2017, **344**, 36-41.
3. K. P. Wang, J. P. Chen, S. J. Zhang, Y. Lei, H. Zhong, S. Chen, X. H. Zhou and Z. Q. Hu, *Analytical and Bioanalytical Chemistry*, 2017, **409**, 5547-5554.
4. W. Wang, Y. Li, P. V. Reddy, X. Zhang and D. Yuan, *Sensors and Actuators B: Chemical*, 2017, **252**, 159-164.
5. S. Chand, M. Mondal, S. C. Pal, A. Pal, S. Maji, D. Mandal and M. C. Das, *New Journal of Chemistry*, 2018, **42**, 12865-12871.
6. Y. Dai, J. J. Zhang, S. Q. Liu, H. Zhou, Y. J. Sun, Y. Z. Pan, J. Ni and J. S. Yang, *Chemistry*, 2018, **24**, 9555-9564.
7. V. Kumar, B. Sk, S. Kundu and A. Patra, *Journal of Materials Chemistry C*, 2018, **6**, 12086-12094.
8. A. Kundu and S. P. Anthony, *Spectrochimica Acta Part A: Molecular and Biomolecular Spectroscopy*, 2018, **189**, 342-348.

9. R. Lv, Z. Chen, X. Fu, B. Yang, H. Li, J. Su, W. Gu and X. Liu, *Journal of Solid State Chemistry*, 2018, **259**, 67-72.
10. H. Yao, J. Wang, S. S. Song, Y. Q. Fan, X. W. Guan, Q. Zhou, T. B. Wei, Q. Lin and Y. M. Zhang, *New Journal of Chemistry*, 2018, **42**, 18059-18065.
11. X. Yue, C. Li and Z. Yang, *Journal of Photochemistry and Photobiology A: Chemistry*, 2018, **351**, 1-7.
12. M. Arici, *New Journal of Chemistry*, 2019, **43**, 3690-3697.
13. S. K. Dinda, A. Upadhyay, S. Polepalli, M. Althaf Hussain and C. P. Rao, *ACS Omega*, 2019, **4**, 7723-7733.
14. Y. Liu, C. Liu, X. Zhang, L. Liu, C. Ge, X. Zhuang, N. Zhang, Q. Yang, Y.-Q. Huang and Z. Zhang, *Journal of Solid State Chemistry*, 2019, **272**, 1-8.
15. M. Orojloo and S. Amani, *Polycyclic Aromatic Compounds*, 2019, **41**, 33-46.
16. Z. Qiao, Y. Wu, B. Tang, R. Perestrelo and R. Bhalla, *Tetrahedron Letters*, 2019, **60**, 150918.
17. M. Zhang, L. Gong, C. Sun, W. Li, Z. Chang and D. Qi, *Spectrochimica Acta Part A: Molecular and Biomolecular Spectroscopy*, 2019, **214**, 7-13.
18. N. Ahfad, G. Mohammadnezhad, S. Meghdadi and H. Farrokhpour, *Spectrochimica Acta Part A: Molecular and Biomolecular Spectroscopy*, 2020, **228**, 117753.
19. H. Guo, N. Wu, R. Xue, H. Liu, L. Li, M. Wang, W. Yao, Q. Li and W. Yang, *Colloids and Surfaces A: Physicochemical and Engineering Aspects*, 2020, **585**, 124094.
20. S. Panja, S. Mondal, S. Ghosh, U. Ghosh and K. Ghosh, *ACS Omega*, 2020, **5**, 13984-13993.
21. S. T. Wang, X. Zheng, S. H. Zhang, G. Li and Y. Xiao, *CrystEngComm*, 2021, **23**, 4059-4068.
22. R. Xu, Q. Wu, C. Xing, H. Wang, W. Xu, X. Meng and H. Hou, *Polyhedron*, 2021, **197**, 115056.
23. D. G. Cai, C. Q. Qiu, Z. H. Zhu, T. F. Zheng, W. J. Wei, J. L. Chen, S. J. Liu and H. R. Wen, *Inorganic Chemistry*, 2022, **61**, 14770-14777.